JOURNAL OF CATALYSIS 71, 257–269 (1981)

Study of the Oxidative Dehydrogenation of Ethylbenzene

I. Catalytic Behavior of SnO_2–P_2O_5

YUICHI MURAKAMI, KAZUYOSHI IWAYAMA, HIROSHI UCHIDA, TADASHI HATTORI, AND TOMOHIKO TAGAWA

Department of Synthetic Chemistry, Faculty of Engineering, Nagoya University, Furo-cho, Chikusa-Ku, Nagoya 464, Japan

Received October 24, 1980; revised May 18, 1981

The oxidative dehydrogenation of ethylbenzene to styrene on SnO_2–P_2O_5 catalyst was investigated and the effects of catalyst composition and calcination temperature were studied. Elimination of phosphoric acid from SnO_2–P_2O_5 catalyst by nitric acid treatment and phosphoric acid treatment of the SnO_2 surface result in an increase of activity and selectivity. The catalytic behavior of SnO_2–P_2O_5 catalysts is compared with that of crystalline tin(IV) phosphate. The interdependence of catalytic activity and selectivity, catalyst crystalline structure, and BET surface area is also discussed. These indicate that a type of tin–phosphorus compound is the active component. Also an increase in activity with reaction time and by calcination is explained. A mechanism consisting of the abstraction of hydrogen from ethylbenzene by surface oxygen to form styrene and the regeneration of oxygen from gas phase to the catalyst surface is proposed, with consideration of the role of tin and phosphorus, on the basis of kinetic data in a differential flow reactor.

INTRODUCTION

Styrene is produced on a commercial scale from ethylbenzene (EB) by a catalytic dehydrogenation reaction in the vapor phase at 600–700°C, just below the region where thermal cracking becomes significant. This is an endothermic reaction affected by an equilibrium which favors the products as the temperature is increased and the pressure reduced. Superheated steam is used as the additive to provide heat needed for the reaction, to reduce the ethylbenzene and hydrogen partial pressures to maximize yields, and to keep the catalyst clean and active. On the other hand, the oxidative dehydrogenation which is an exothermic reaction, can make the equilibrium shift toward the desired product, lower the reaction temperature, and reduce the volume of the steam diluent required by feeding oxygen with reactant. This oxidative dehydrogenation process is currently increasing in importance and a catalyst which shows high activity and selectivity is now desired (*1*). The direct oxidation of hydrocarbons to get oxygen-containing products has been developed as have some oxidation processes such as ammoxidation and oxychlorination which have been used on the industrial scale. These situations suggest the possibility of producing styrene by the oxidative dehydrogenation process, thus saving energy. However, the selectivity is not sufficient in the oxidative dehydrogenation of ethylbenzene on the bismuth–molybdenum catalyst (*2*) which is one of the typical mild oxidation catalysts for the production of the commercial base.

In our screening study (*3*) the activity and selectivity of various oxide catalysts were examined, and SnO_2–P_2O_5 catalyst was found to show both high yield and high selectivity to styrene. In the present study, further investigations were carried out on SnO_2–P_2O_5 catalyst. The state and the role of the phosphorus were investigated by X-ray diffraction and chemical treatment of the catalyst. The active component is dis-

0021-9517/81/100257-13$02.00/0

cussed comparing it with crystalline tin phosphate. The mechanism of the activation of oxygen and ethylbenzene on the catalyst is also discussed on the basis of kinetic data in a differential flow reactor and by the pulse reaction technique.

EXPERIMENTAL

Catalysts

Tin oxide (SnO_2), solid phosphoric acid catalyst (Solid-P), and SnO_2–P_2O_5 (Sn–P) were prepared by the method reported in our screening study (*3*). Crystalline tin(IV) phosphate (c-SnP) was prepared by the method of Costantino and Gasperoni (*4*). Anhydrous tin(IV) chloride was added to 1.6 liter of 8 *M* H_3PO_4 and 3 *M* HNO_3 until the P : Sn ratio reached 30 and then the solution was refluxed for 100 h. The product was then washed with distilled water until pH 4 was obtained, dried under vacuum at room temperature for several days, pressed, and sieved. The BET surface areas of c-SnP were 13.1 and 5.9 after being calcined at room temperature and 550°C, respectively. The X-ray diffraction pattern of the c-SnP thus obtained was in good agreement with that previously reported (*4*).

Flow Reaction

The continuous flow reaction was carried out with conventional fixed-bed equipment at atmospheric pressure using a Pyrex reactor with an i.d. of 10 mm, at the center of which a Pyrex tube with an o.d. of 4 mm was installed as a cover for the thermocouple. The catalyst particles were dispersed in fused alumina particles to prevent a local increase of the temperature and packed in the reactor. The reactor was installed in an electrically heated fluidized sand bath in order to heat the catalyst bed uniformly. A stream of ethylbenzene vapor, steam, and oxygen was fed after dilution with nitrogen. A contact time (W/F) of 21.6 g · h/mol, and a reaction temperature (T) of 450°C were used in these experiments unless otherwise stated. Other reaction conditions, such as catalyst weight (W), partial pressures of ethylbenzene (P_{EB}), oxygen (P_{O_2}) and steam (P_{H_2O}) are indicated in the respective figures and tables. The liquid products were trapped in an ice bath and a dry ice–acetone bath. The gaseous products were sampled at the outlet of the reactor. Peroxides in ethylbenzene were removed by a silica gel column.

Conversion, yield, and selectivity are shown in the following equations:

$$\text{ST selectivity} = (\text{ST formed/EB reacted}) \times 100,$$
$$\text{EB conversion} = (\text{EB reacted/EB fed}) \times 100,$$
$$\text{ST yield} = (\text{ST formed/EB fed}) \times 100,$$
$$\text{CO} + \text{CO}_2 \text{ yield} = (\text{CO} + \text{CO}_2 \text{ formed/EB fed} \times 8) \times 100,$$
$$\text{B yield} = (\text{B formed/EB fed}) \times 100,$$

ST = styrene, EB = ethylbenzene, B = benzene.

Analysis

The analysis of the products was carried out with gas chromatography. The analysis of gaseous products (O_2, N_2, CO, and CO_2) was performed by the intermediate-cell method (*2*, *5*) with a 25-cm silica gel + 25-cm activated-carbon column at 110°C and a 2-m MS 13X column at room temperature. The liquid products were analyzed by a 2-m DOP column at 110°C with bromobenzene as an internal standard.

Pulse Reaction

Pulse equipment shown in Fig. 1 was used with oxygen-free helium as the carrier gas (Cu–Zn catalyst, Nikki Chemical Company, Ltd. N-211, reduced by H_2 was used at 300°C to remove oxygen) (*6*). The pulse size was 1 μl and the analysis of recovered ethylbenzene and the products (styrene, benzene, toluene, CO, and CO_2) was performed by the intermediate-cell method (*5*) with a 2-m PEG (30% on C-22) + 0.5-m

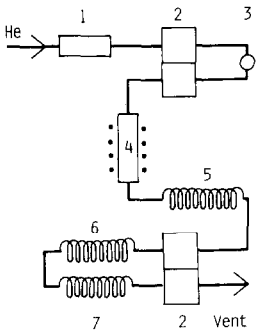

FIG. 1. Reactor system for the pulse studies. (1) Reduced Cu–Zn catalyst for removing oxygen, (2) thermal-conductivity detector, (3) sample inlet, (4) reactor containing 250 mg of catalyst in an electrically heated Pyrex glass tube with an i.d. of 5 mm, (5) chromatographic column, PEG (2 m) + DOP (0.8 m), (6) chromatographic column, activated carbon (1.5 m), (7) empty tube.

DOP (30% on C-22) column and a 1.5-m activated-carbon column with an adequate empty tube to control the retention time. Another TCD cell was installed to determine the amount of ethylbenzene pulsed before the reactor.

RESULTS

As shown in Table 1, the Sn–P catalyst showed higher yield of styrene than the SnO_2 and Solid-P catalysts. SnO_2 showed high yield of CO and CO_2 but poor yield of styrene. Solid-P showed high selectivity but poor activity.

Effect of Composition of the Sn–P Catalyst

The effect of amounts of phosphoric acid in the Sn–P catalyst on the catalytic activity and selectivity was studied. As shown in Fig. 2, the EB conversion and ST yield increased for values of phosphoric acid below 9%, decreased above it, and was constant for values above 15%, while the CO + CO_2 yield decreased for values of phosphoric acid below 15% and remained constant for values above it. Thus the ST selectivity increased from 36.1 to 90% below 9 at.% of phosphoric acid and, above 9 at.%, remained constant at 90%. The change of surface area resembled that of ST yield.

TABLE 1

Activity and Selectivity of Sn–P Compared with SnO_2 and Solid-P[a]

Catalyst[b]	EB conversion (%)	ST selectivity (%)	Yield of CO + CO_2 (%)	$\frac{CO}{CO_2}$
SnO_2	17.7	39.1	4.6	0.09
Sn–P (P, 9 at.%)	32.1	83.3	2.1	0.95
Solid-P	16.5	88.5	0.7	0.86

[a] $P_{EB} : P_{O_2} : P_{H_2O} = 0.133 : 0.100 : 0.313$ atm.
[b] Catalysts are the same as those screened elsewhere (*3*).

Effect of Calcination Temperature

The effect of calcination temperature is shown in Fig. 3. The Sn–P (P, 9 at.%) was calcined at 500°C for 2 h in air, and then calcined again at 600, 700, and 1000°C for 2 h. High calcination temperatures resulted in low yields of carbon oxides and benzene. On the other hand, the ST yield and BET

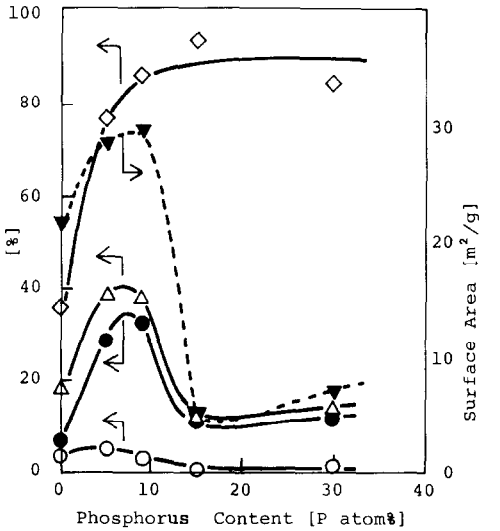

FIG. 2. Effect of phosphoric acid contents on ST selectivity (◇), EB conversion (△), ST yield (●), CO + CO_2 yield (○), and BET surface area (▼). P_{EB} = 0.100 atm, P_{O_2} = 0.100 atm, P_{H_2O} = 0.313 atm.

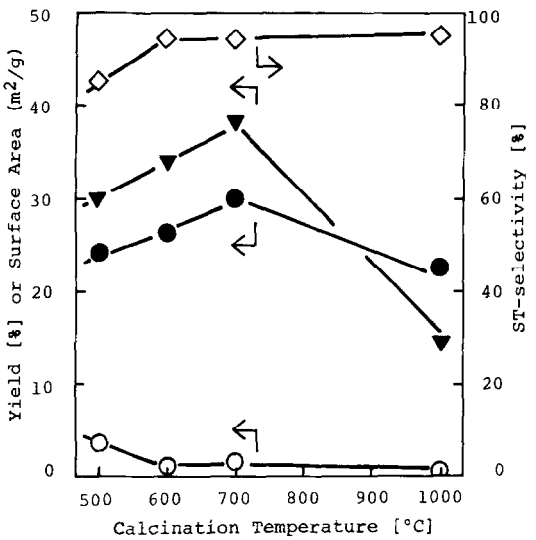

FIG. 3. Effect of calcination temperature on Sn–P (P, 9 at.%) catalyst. P_{EB} = 0.200 atm, P_{O_2} = 0.100 atm, P_{H_2O} = 0.000 atm. For the symbols, see Fig. 2.

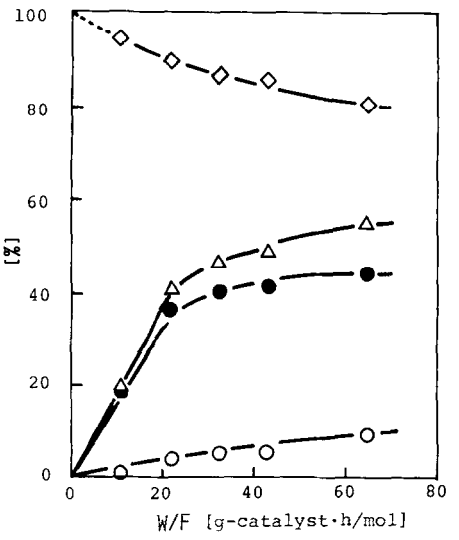

FIG. 4. Effect of feed rate on Sn–P (P, 9 at.%) catalyst calcined at 1000°C for 4 h. W = 4.5 g, P_{EB} = 0.200 atm, P_{O_2} = 0.25 atm, P_{H_2O} = 0.000 atm. For the symbols, see Fig. 2.

surface area increased until 700°C and decreased above 700°C. The ST selectivity also slightly increased.

Effect of Reaction Conditions

The effect of steam co-feeding in the flow reaction is shown in Table 2. The presence of steam reduced the total oxidation to one-third of that observed in the absence of steam. A corresponding amount of styrene was recovered in the presence of steam, which increased the selectivity without reducing the conversion of ethylbenzene.

The effect of the total feed rate (F) under the conditions, W = 4.5 g, P_{EB} = 0.20 atm, and P_{O_2} = 0.25 atm, is shown in Fig. 4. The decrease in W/F to zero resulted in ST selectivity as high as 100%.

TABLE 2

Effect of Steam on the Oxidative Dehydrogenation of Ethylbenzene[a]

P_{H_2O}[b] (atm)	Yield (%)				EB conversion (%)	ST Selectivity (%)
	$CO + CO_2$	B	T	ST		
0.000	3.5	0.9	0.1	23.9	28.3	84.3
0.313	1.2	1.1	0.2	25.5	27.9	91.3

[a] Catalyst: Sn–P (P, 9 at.%) calcined at 500°C for 2 h, 4.5 g.
[b] P_{EB}: P_{O_2} = 0.200 : 0.100 atm.

Reaction in the Differential Reactor

Oxygen partial pressure was varied with constant P_{EB} at 0.15 atm and ethylbenzene partial pressure was varied with constant P_{O_2} at 0.20 atm under the following conditions: reaction temperature = 450°C, total feed = 290 mmol/h, and catalyst weight = 0.50 g (Sn–P, P = 9 at.% calcined at 1000°C for 24 h). The catalyst was diluted with 8.0 g of fused alumina. The partial pressure was varied at random to avoid the influence of the change of catalytic activity with time. Under these conditions, the conversion is so low that the partial pressure in the catalyst bed can be regarded as constant. As shown in Fig. 5, the apparent reaction orders with respect to the pressure of ethylbenzene and oxygen were 0.60 and 0.47, respectively. Considering that the oxidation and oxidative dehydrogenation of olefins on the Bi–Mo catalyst have been reported to show reaction orders of 1.0 and 0.0, respectively, with respect to the pressure of olefin and oxygen, the coverage of oxygen on Sn–P can be considered to be

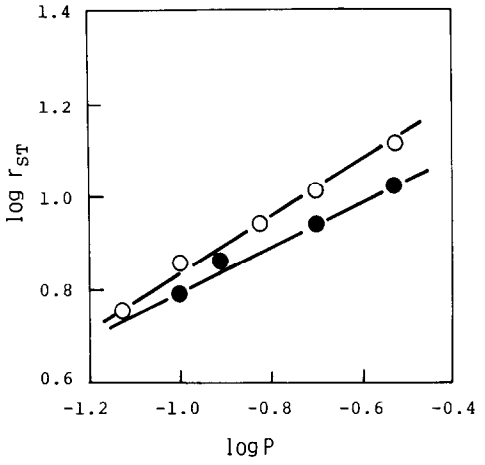

FIG. 5. Effect of partial pressure on the rate of styrene formation in the differential reactor on Sn–P (P, 9 at.%) catalyst calcined at 1000°C for 4 h. P_{O_2} was changed with P_{EB} = 0.15 atm (○) and P_{EB} was changed with P_{O_2} = 0.200 atm (●). W/F = 1.72 g · h/mol, P_{H_2O} = 0.000 atm.

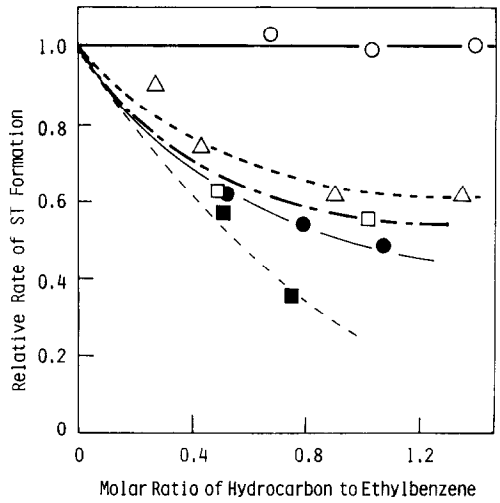

FIG. 6. Competitive reaction on Sn–P (P, 9 at.%) catalyst calcined at 1000°C for 4 h. Relative rate of styrene formation = r_{ST} in the presence of hydrocarbons/r_{ST} in the absence of hydrocarbons. W/F = 1.81 g · h/mol, P_{EB} = 0.100 atm, P_{O_2} = 0.100 atm, P_{H_2O} = 0.339 atm. Hydrocarbons: benzene (○), isopropylbenzene (△), *o*-xylene (□), toluene (●), *p*-xylene (■).

not so high in the present reaction. This is similar to that reported on the oxidation of propylene on Sn–Sb catalyst, which too was said to depend on the oxygen partial pressure (*7*).

Change of Activity with Reaction Time

The activity increased gradually with time in these experiments on the Sn–P catalysts. This increment differed with P content, calcination temperature, and reaction conditions. For example, under the conditions, reaction temperature = 450°C, W/F = 34.5 g-cat · h/mol, P_{EB} = 0.14 atm, P_{O_2} = 0.10 atm, P_{N_2} = 0.44 atm, and P_{H_2O} = 0.32 atm on Sn–P catalyst (P, 9 at.%, calcined at 600°C for 2 h), the ST yield increased from 19.5% at 1 h, to 23.0% at 11 h, although the ST selectivity did not change as much.

Inhibition of Reaction

Figure 6 shows the competitive reaction of ethylbenzene with other aromatic hydrocarbons. The rate of styrene formation in the presence of hydrocarbons was compared with that in the absence of hydrocarbons as a function of the molar ratio of the hydrocarbon added to ethylbenzene. Alkylbenzenes such as isopropylbenzene, *o*-xylene, toluene, and *p*-xylene reduced the rate of styrene formation to one-half of that in their absence, while the presence of benzene did not change the rate. These results suggest the importance in this reaction, of alkyl groups which possess hydrogen at the α position.

Pulse Reactions

Styrene, benzene, and carbon oxides were formed when only ethylbenzene was pulsed on SnO_2 and Sn–P (P, 9 at.%) which were calcined at 500°C. In the helium carrier which contained a slight amount of oxygen (about 20 ppm), styrene and the other products were formed by every pulse of ethylbenzene. However, as shown in Fig. 7, in the oxygen-free helium, products became undetectable after some pulses of ethylbenzene had been performed, but a pulse of oxygen (10 ml) regenerated the activity. In the cases of Bi–Mo shown in Fig. 8 and other oxide catalysts, the forma-

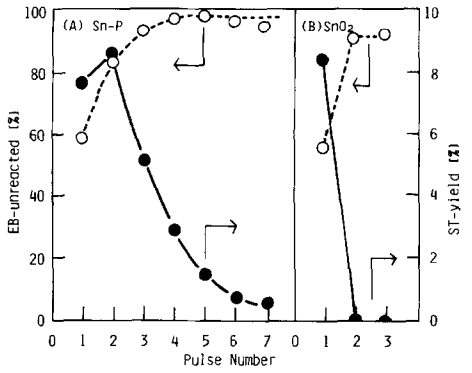

FIG. 7. Effect of pulse number on Sn–P (P, 9 at.%) (A) and on SnO_2 (B) catalysts in the pulse reaction at 460°C. Catalysts: calcined at 500°C for 2 h, 250 mg. Pulse size: ethylbenzene 1 μl with 20-min interval. ST yield (●), EB unreacted (○) which was recovered after the pulse reaction.

tion of sytrene did not decrease steeply as these catalysts were reduced with pulses of ethylbenzene in the oxygen-free helium. This was similar to the case of oxygen-containing helium.

On the Solid-P catalyst, products from ethylbenzene pulse were not detected even after a pulse of oxygen (10 ml), irrespective of the presence or absence of about 20 ppm of oxygen in the carrier gas. However, the recovery of ethylbenzene was insufficient and the amount unrecovered was about 15% for each pulse of ethylbenzene.

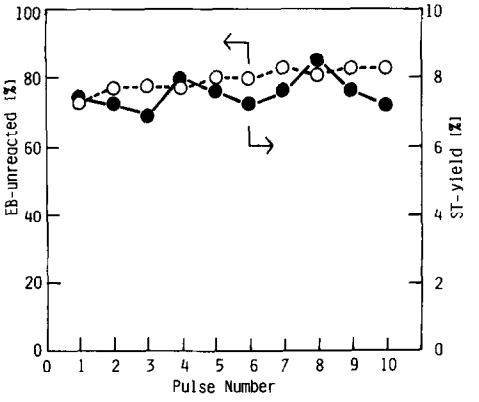

FIG. 8. Effect of pulse number on Bi–Mo catalyst in the pulse reaction at 460°C. For the reaction conditions and the symbols, see Fig. 7.

Effect of Treatment of SnO_2 with Phosphoric Acid

Tin dioxide was calcined at 1000°C for 4 h and impregnated with phosphoric acid, boiled for 4 h, washed, and calcined at 500°C for 2 h. As shown in Table 3, this catalyst showed high ST yield, high ST selectivity, and little combustion, similar to the Sn–P catalyst prepared from $Sn(OH)_2$ and phosphoric acid. As X-ray diffraction pattern and BET surface area of this catalyst showed little change, this treatment with phosphoric acid is considered to modify the surface of SnO_2.

Effect of Various Treatments of the Sn–P Catalyst

The various methods of chemical treatment of Sn–P (P, 15 at.%) calcined at 500°C and the results of the reaction on these catalysts are shown in Table 4 along with their specific surface areas. Styrene yield and ST selectivity were not changed after being left in water for 3 days but increased a little after being left in boiling water for 11 h. Such increments in ST yield and ST selectivity were apparent after being treated in boiling 3.6 N HNO_3 for 10 h. These results are, considering the increase of BET surface area and elution of phosphoric acid from the catalyst detected by

TABLE 3

Change of Tin Dioxide Surface Properties by Phosphoric Acid Treatment[a]

	SnO_2[b]	
	Untreated	Treated by H_3PO_4
EB conversion (%)	15.3	17.4
ST yield (%)	4.92	14.9
B yield (%)	5.09	0.64
CO + CO_2 yield (%)	5.24	1.68
ST selectivity (%)	32.2	85.6
Surface area (m^2/g)	4.1	4.0

[a] W/F = 15.5 g · h/mol, T = 450°C, $P_{EB} : P_{O_2} : P_{N_2} : P_{H_2O}$ = 0.14 : 0.14 : 0.40 : 0.32 atm.
[b] Precalcined at 1000°C for 4 h, W = 4.5 g.

TABLE 4

Effect of Elimination of Phosphoric Acid by Various Treatments[a]

Treatment	ST yield (%)	ST selectivity (%)	Surface area (m^2/g)
Untreated	13.0	87.5	4.65
In water for 3 days	13.2	87.7	5.04
In boiling water for 11 h	15.7	89.4	5.61
In boiling 3.6 *N* HNO_3 for 10 h	21.9	92.1	6.38

[a] Catalyst: Sn–P (P, 15 at.%) calcined at 500°C, W/F = 15.5 g · h/mol, $P_{EB}:P_{O_2}:P_{N_2}:P_{H_2O}$ = 0.071 : 0.14 : 0.47 : 0.32 atm.

magnesia mixture, attributable to the elimination of excess phosphoric acid which covered the active surface.

The results of treatment of Sn–P (P, 9 at.%) calcined at 600 and 700°C are shown in Table 5. The treatment in boiling 3.6 *N* HNO_3 increased ST yield from 13.2 and 14.2% to 16.1 and 17.4% on the catalysts calcined at 600 and 700°C, respectively. Styrene-yield on the sample calcined at 700°C was still higher after the HNO_3 treatment than that on the sample calcined at 600°C. The effect of HNO_3 treatment before the reaction and that after the reaction for 11 h were relatively the same.

X-Ray Diffraction Experiment

In the X-ray diffraction patterns of SnO_2 and Sn–P (P, 9 at.%) catalysts calcined at various temperatures, lines other than SnO_2 could not be observed and changes in the lattice constant were not observed. The crystal size D and strain η calculated from the diffraction patterns are shown in Table 6. When the Sn–P catalyst was calcined at 700°C, the crystal size did not change appreciably, but the strain decreased and the specific surface area increased as shown in Fig. 3. When calcined at 1000°C, the crystal size increased and the surface area decreased. In the case of the SnO_2 catalyst, the growth of the crystal was greater and the strain was less than those of the Sn–P catalysts.

Fluorescent X-Ray Experiment

The intensity of phosphorus in the fluorescent X-ray spectra of Sn–P (P, 9 at.%) catalysts calcined at 600°C is shown in Table 5. The amount of phosphorus decreased after the HNO_3 treatment to 80% of the fresh state, and the same amount of the decrement was observed by the HNO_3 treatment of the sample after being used in the flow reaction.

Behavior of Crystalline Tin Phosphate

For further investigation on the cooperative effect of tin and phosphorus, oxidative

TABLE 5

Change of Catalysts by Nitric Acid Treatment[a]

Calcination (°C)	Treatment	ST yield (%)	ST selectivity (%)	P amount[b] (a.u.)
600	Untreated	13.2	94.1	1801
	Boiling in 3.6 *N* HNO_3 for 23 h	16.1	88.6	1436
	Boiling in 3.6 *N* HNO_3 for 23 h after 11 h reaction	14.2	89.9	1520
700	Untreated	14.2	95.4	—
	Boiling in 3.6 *N* HNO_3 for 23 h	17.4	89.7	—

[a] Catalyst: Sn–P (P, 9 at.%), T = 450°C, W/F = 15.5 g · h/mol, $P_{EB}:P_{O_2}:P_{N_2}:P_{H_2O}$ = 0.14 : 0.10 : 0.44 : 0.32 atm.

[b] Intensity of phosphorus ($PK\alpha$) in the fluorescent X-ray spectrum.

TABLE 6

Size and Strain of SnO_2 Crystals in Catalysts[a]

Catalyst	Calcination Temp. (°C)	Crystal Size, D (Å)	Strain η
Sn–P	500	170	0.0045
(P, 9 at.%)	700	180	0.0019
	1000	350	0.0010
SnO_2	500	280	0.0022
	1000	2600	0.0006
	500[b]	240	0.0040

[a] X-Ray diffraction patterns were obtained by Rigaku Denki diffractometer, Model Geigerflex with Cu$K\alpha$ radiation.

[b] Boiled in H_3PO_4.

dehydrogenation of ethylbenzene on the crystalline tin(IV) phosphate (c-SnP) was carried out. The activity of c-SnP was a little lower than that of the Sn-P catalyst and the selectivity was as high as that of the latter. As shown in Fig. 9, the ST yield on the uncalcined c-SnP increased with time. Reoxidation of c-SnP resulted in a further increase in the ST yield. On the other hand, the ST yield on c-SnP calcined at 550°C for 2 h remained constant and was almost equivalent to that on the uncalcined c-SnP after the reoxidation.

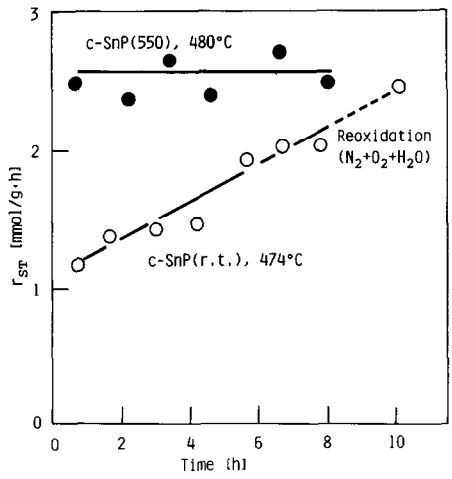

FIG. 9. Change of activity with reaction time on c-SnP catalyst. P_{EB} = 0.158 atm, P_{O_2} = 0.196 atm, P_{H_2O} = 0.217 atm. T = 480°C for c-SnP calcined at 550°C for 2 h (●); T = 474°C for c-SnP uncalcined (r.t.) (○).

DISCUSSION

Reaction Mechanism

A π-allyl mechanism is generally accepted in the oxidation of olefins. Sachtler and DeBoer have reported that the rate-determining step of propylene oxidation is the dissociative adsorption of propylene by the cleavage of the C–H bond in the methyl group of propylene in the ^{14}C-tracer studies (*8*). Similar results have been obtained on Cu_2O catalyst (*9*) and phosphorus-containing Bi–Mo catalyst (*10, 11*). The reactions of deuterated propylene on Cu_2O, Bi–Mo, and U–Sb also suggest the existence of the π-allyl intermediate (*12–14*). Such an intermediate has also been observed on ZnO catalyst by ir studies (*15*). A similar allylic intermediate has been proposed in the oxidative dehydrogenation of butenes on Bi–Mo (*16*) and ferrite catalysts (*17*) and the abstraction of a hydrogen in the allyl position has been concluded to determine the rate of this reaction.

The competitive reaction also suggests the importance of the α hydrogen of ethylbenzene. As shown in Fig. 6, the relative rate of ST formation in the inhibition of the reaction decreased with some aromatic compounds but not with benzene. The relative rate decreased with the increment of the amount of the inhibitor and decreased in the order: None = benzene > isopropylbenzene > *o*-xylene > toluene > *p*-xylene. This order of inhibition is in good agreement with the enthalpies of heterolysis of hydrogen as follows (kcal/mol): phenyl (300) ≫ benzyl (247) > *p*-methylbenzyl (240) (*18*). Inhibitors such as toluene and xylenes do not react in this reaction, showing that this inhibition is due to the competitive adsorption of ethylbenzene and the inhibitor. These results suggest that ethylbenzene is adsorbed by the abstraction of α hydrogen on the catalyst.

In the oxidative dehydrogenation of eth-

ylbenzene, one of the most probable mechanisms is one which consists of abstraction of hydrogen from ethylbenzene by the lattice oxygen on the surface to form styrene, and reoxidation of the catalyst by gas-phase oxygen (*19*).

$$EB + [O] \xrightarrow{k_1} ST + [\ ], \quad (1)$$

$$[\ ] + \tfrac{1}{2} O_2 \xrightarrow{k_2} [O], \quad (2)$$

where [O] represents the lattice oxygen at the surface layer of the catalyst because the bulk oxygen has been reported to be inactive (*20*), which is in good agreement with the results of pulse reaction shown in Fig. 7. The rates of (1) and (2) are

$$r_1 = k_1 P_{EB} \theta, \quad (3)$$

$$r_2 = k_2 P_{O_2} (1 - \theta). \quad (4)$$

As $r_1 = r_2$ in the steady state, the rate of styrene formation is given as

$$r = \frac{k_1 k_2 P_{EB} P_{O_2}}{k_1 P_{EB} + k_2 P_{O_2}}, \quad (5)$$

$$\frac{1}{r} = \frac{1}{k_1 P_{EB}} + \frac{1}{k_2 P_{O_2}}. \quad (6)$$

The reciprocal relationship between $1/r$ and $1/P$ is shown in Fig. 10. The rate constants k_1 and k_2 calculated from the slope of the plot of $1/r$ against $1/P_{O_2}$ in Fig. 10 were 108 and 101, and were 101 and 109 (mmol/g-cat · atm · h) from the plot of $1/r$ against $1/P_{EB}$. The rate constants from both plots agreed very well with one another and oxidative dehydrogenation of ethylbenzene proceeds along the proposed reduction–oxidation mechanism.

The fraction of oxidized site (θ) was about 0.5 so that the surface of the catalyst was more reduced than that of the Bi–Mo catalyst, θ of which has been reported to be about 1.

Effect of Steam

The apparent effect, shown in Table 2, of the presence of steam is to release the styrene formed to the gas phase without side reactions. Steam may inhibit the re-

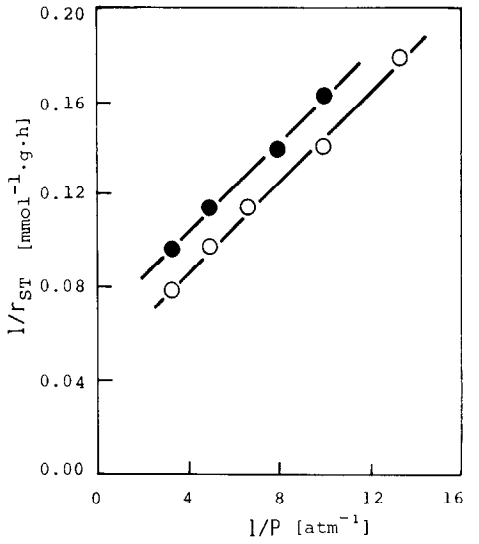

FIG. 10. Reciprocal relations between rate and partial pressure. For the reaction conditions and the symbols, see Fig. 8.

adsorption of styrene on the catalyst which results in the inhibition of further reaction of styrene to increase the selectivity.

Effect of Phosphorus

One of the reasons for high activity of Sn–P is the inhibition of the growth of SnO_2 crystal by the addition of phosphorus as shown in Table 6. The crystal size of SnO_2 increased up to 280 and 2600 Å, when $Sn(OH)_2$ was calcined at 500 and 1000°C, respectively. With an addition of 9 at.% of phosphoric acid, the crystal size of SnO_2 was 170 Å when calcined at 500°C and was only 350 Å after calcination at 1000°C.

On the other hand, not only the catalytic activity, but also the yield of by-products and the CO/CO_2 ratio were different between Sn–P and SnO_2 catalysts.

As is shown in Fig. 4, decreasing W/F to zero results in 100% ST selectivity on the Sn–P catalyst, but the selectivity does not appear to reach 100% on the SnO_2 catalyst. This shows that one of the effects of phosphorus is to inhibit the reaction to form by-products from ethylbenzene, because the by-products are formed from ethylbenzene and styrene in the case of the SnO_2 catalyst,

but mainly from styrene in the case of the Sn–P catalyst. These results show the essential difference between the effective sites of the SnO_2 and Sn–P catalysts.

The X-ray diffraction studies showed that phosphorus does not exist in the SnO_2 crystal but rather on the surface of the SnO_2 crystal, because other diffraction peaks except for SnO_2 were not detected: Nor was any change in the lattice constant in any Sn–P catalyst detected.

The increase of activity and selectivity by water or nitric acid treatments indicates that the effective site did not dissolve into the water or the nitric acid, while an inactive substance covering the catalyst surface is removed. $Sn_2O(PO_4)_2$ prepared from tin(II) chloride treated by phosphoric acid is known not to be dissolved in nitric acid (*21*). The excess methaphosphoric acid is eliminated into the liquid phase which was detected by magnesia solution and the amount of phosphorus decreased was about 20% as shown in Table 5. The phosphoric acid treatment of SnO_2, prepared by the calcination of $Sn(OH)_2$, changed the selectivity despite the constant value of the BET surface area (Table 3) and the catalytic action resembles, but is a little lower in yield and selectivity, that of catalysts which were prepared by adding the phosphoric acid directly into $Sn(OH)_2$. The catalytic activity of Sn–P COMPD prepared from tin(II) chloride and phosphoric acid was not so high, while the selectivity was satisfactory (*3*). Moreover, the increase in activity and selectivity by the removal of free phosphoric acid shows that the free phosphoric acid on the catalyst surface is not the active component. From these results, the effective active site of Sn–P catalyst can be attributed to the surface Sn–P compounds such as tin phosphate.

Origin of Change in Activity with Time and Calcination Temperature

Reasons for the increase of activity with time in the reaction or with the calcination temperature could be (1) the vaporization of free phosphoric acid on the surface to make the active site exposed and (2) the reaction of SnO_2 with phosphoric acid to increase the amount of the active Sn–P compounds on the surface.

Styrene yield on fresh catalyst was 13.2% and nitric acid treatment increased the value to 16.0%. Nitric acid treatment of the catalyst which had been used for 11 h in the flow reaction gave a 16.1% ST yield. This is in good agreement with the P content determined by fluorescent X-ray studies as shown in Table 5. These results indicate that the activity increases due to reason (1), but that the reaction of SnO_2 with phosphoric acid to form active compounds does not occur during the oxidative dehydrogenation for 11 h.

Comparing the catalysts calcined at 600 and 700°C (Table 4), the crystal sizes were constant and the latter catalyst showed a higher ST yield even after the removal of free phosphoric acid by nitric acid treatment. This increment with the increase of calcination temperature is attributable to reason (2) and will be discussed in the following section.

Behavior of Crystalline Tin Phosphate

As the effective active site on the Sn–P catalyst is attributed to surface compounds such as tin phosphate, the details of the catalytic behavior of c-SnP were studied.

The results of the c-SnP catalysts shown in Fig. 9 indicate that the increase in the ST yield on the uncalcined c-SnP is caused by the change of the structure of the c-SnP during the reaction. This change could be assumed not to be caused by the loss of free phosphoric acid due to the following reasons: (1) c-SnP is considered not to contain excess phosphoric acid on the surface, (2) loss of phosphorus is little in the case of c-ZrP catalyst (*22*). The X-ray diffraction pattern of the uncalcined c-SnP used in the reaction was different from that of the fresh c-SnP, but identical to that of the calcined

c-SnP. The specific reaction rate of styrene formation on the calcined c-SnP was 0.30 and 0.38 mmol · h^{-1} · m^{-2} at 450 and 480°C, respectively. These values are in good agreement with those on Sn–P catalysts calcined at 600°C: 0.27–0.32 mmol · h^{-1} · m^{-2} at 450°C. This result shows that the surface structure of Sn–P catalyst is similar to that of the calcined *c*-SnP.

At present, the crystal structure of c-SnP is not clear, but the similarities in the preparation method and the X-ray diffraction pattern suggest that the structure of c-SnP also is similar to that of c-ZrP (*23*). Crystalline zirconium phosphate is dehydrated in two steps (*22, 24*); the crystalline water is dehydrated at 130°C and the structure water is dehydrated at 500–600°C. DSC measurement was carried out to examine the dehydration process of c-SnP. The first mole of water was dehydrated at 130°C similarly to c-ZrP. But the dehydration of the second mole of water appeared to start at a lower temperature than c-ZrP. The dehydration was almost complete at 550°C. Usually, the dehydration of orthophosphate is accompanied by the condensation of phosphate to form pyrophosphate. However, the X-ray diffraction pattern of the calcined c-SnP was different from that of tin pyrophosphate, but similar to that of the unidentified phase of c-ZrP obtained by the calcination of c-ZrP at 600°C (*22, 24*). Thus, c-SnP calcined at 550°C can be regarded as the dehydrated but noncondensed state. Such an unstable state would result in the formation of new active sites.

As described elsewhere (*22*) both uncalcined and calcined c-ZrP have the acid site with the acid strength of $+4.8 > H_0 > +3.3$ and $-3.0 > H_0 > -5.6$, and the acidity is attributed to the phosphate group. Thus, the calcination does not appear to modify the phosphate group. The same would be true in the case of c-SnP. The calcination of c-SnP would not modify the phosphate group which is the origin of the acidity, but would modify the state of the tin atom to form the new active site which may be active oxygen.

Role of Tin and Phosphorus Component

As mentioned above, styrene was formed from the pulse of ethylbenzene without gas-phase oxygen, and styrene was not formed after several pulses of ethylbenzene on SnO_2 and Sn–P catalysts in oxygen-free helium. These facts show that the active oxygen species are held on the catalyst even in the absence of gaseous oxygen and that the surface oxygen, once consumed by the reaction, is not supplied by the diffusion of bulk oxygen. On the other hand, the formation of styrene by every pulse of ethylbenzene in the oxygen-containing helium carrier shows that the surface oxygen once consumed by the reaction, is supplied by the adsorption of gaseous oxygen and that these catalysts can activate oxygen at very low partial pressure such as 20 ppm. This is probably related to the large values of 70.4 and 62.7 kcal/mol in the change of enthalpy and Gibbs free energy, respectively, in the change: $SnO \rightarrow SnO_2$.

On the Solid-P catalyst, reaction did not occur but the constant amount of unrecovered ethylbenzene was observed with every pulse of ethylbenzene. This shows the relatively strong reversible adsorption of ethylbenzene and the weak adsorption of oxygen (*25*).

In the flow of oxygen-free helium, combustion as well as styrene formation was apparent in the first pulse of ethylbenzene on SnO_2 catalyst, but the activity disappeared by the next pulse of ethylbenzene. On the other hand, styrene was formed selectively in the several pulses of ethylbenzene on the Sn–P catalysts. These results agree with the results of the differential conditions. That is, the total oxidation occurs from styrene once formed by the oxidative dehydrogenation on Sn–P catalysts while it occurs both from styrene and ethylbenzene on SnO_2 catalyst. These results suggest that the addition of phosphorus produces not only an enhancement

of the activation of ethylbenzene but is also effective in controlling the nature of the active oxygen which is related to basicity. The strongly activated oxygen on the SnO_2 catalyst, which is active enough for the total oxidation, would be weakened for suitable strength to abstract the hydrogen from ethylbenzene and not strong enough for combustion by the addition of phosphorus.

On the Sn–P catalyst, it seems that Sn, the basic component, contributes to the increase of activity by the adsorption of oxygen and the supply of it to the surface reaction and that P, the acidic component, contributes to the adsorption of ethylbenzene in the active form for this reaction. Also, taking into account the results of c-SnP catalyst in addition to the above discussion, one may consider the mutual interaction of Sn and P to effect an increase in the selectivity of the oxidative dehydrogenation reaction.

This explains well the difference in the catalytic behavior of SnO_2, Solid-P, and Sn–P in the continuous flow reaction.

It is noteworthy that in this study as well as in our screening study (*3*), the acid–base properties of the catalyst have been shown to modify the activity and the selectivity. Hence these relationships could help to clarify the reaction mechanism and to design effective catalysts (*26*). The details of the relationships between the catalytic behavior and the acid–base properties will be discussed in subsequent papers.

CONCLUSION

The addition of phosphorus to SnO_2 catalyst increased the activity and selectivity and effected the prevention of the side reaction from ethylbenzene and the inhibition of the growth of the SnO_2 crystal. The activity and selectivity varied with the catalyst composition and the calcination temperature, and were maximized at a 10-to-1 Sn/P ratio and at a calcination temperature of 700°C. They also increased with some chemical treatments. HNO_3 solution did not dissolve the active site but dissolved away the excess free phosphoric acid which was concentrated at the surface and covered the active site. Such an active site was also generated by the phosphoric acid treatment of the SnO_2 surface. The similarity of the catalytic behavior of Sn–P catalyst to that of crystalline tin(IV) phosphate indicates the active component to be a type of Sn–P compound. A reduction–oxidation mechanism is proposed on the basis of kinetic data in a differential flow reactor. It is suggested that tin, the basic component, activates oxygen and that phosphorus, the acidic component, activates ethylbenzene.

ACKNOWLEDGMENTS

The research was supported in part by a grant from the Asahi Glass Foundation for Contribution to Industrial Technology. The authors thank Mr. H. Hanai for some of the c-SnP studies.

REFERENCES

1. Kaeding, W. W., *Catal. Rev.* **8**, 307 (1974).
2. Murakami, Y., Niwa, M., and Uchida, H., *Kogyo Kagaku Zasshi* **72**, 2183 (1969).
3. Murakami, Y., Iwayama, K., Uchida, H., Hattori, T., and Tagawa, T., to be submitted.
4. Costantino, U., and Gasperoni, A., *J. Chromatogr.* **51**, 289 (1970).
5. Murakami, Y., *Bull. Chem. Soc. Japan* **32**, 316 (1959).
6. Murakami, Y., *Shokubai* **7**, 120 (1965).
7. Hucknall, D. J., "Selective Oxidation of Hydrocarbons," p. 44. Academic Press, New York, 1974.
8. Sachtler, W. M. H., and DeBoer, N. H., *in* "Proceedings, 3rd International Congress on Catalysis, Amsterdam, 1964," p. 252. North-Holland, Amsterdam, 1965.
9. Voge, H. H., Wagner, C. D., and Stevenson, D. P., *J. Catal.* **2**, 58 (1963).
10. McCain, C. C., Gough, G., and Godin, G. W., *Nature* **198**, 989 (1963).
11. Dozono, T., Thomas, D. W., and Wise, H., *J. Chem. Soc. Faraday Trans. I* **69**, 620 (1973).
12. Adams, C. R., and Jennings, T. J., *J. Catal.* **2**, 63 (1963).
13. Adams, C. R., and Jennings, T. J., *J. Catal.* **3**, 549 (1964).
14. Grasselli, R. K., and Suresh, D. D., *J. Catal.* **25**, 273 (1972).
15. Dent, A. L., and Kokes, R. J., *J. Amer. Chem. Soc.* **92**, 6709, 6718 (1970); Dolejsék, Z., and Nováková, J., *J. Catal.* **37**, 540 (1975).

16. Batist, Ph. A., Lippens, B. C., and Schuit, G. C. A., *J. Catal.* **5**, 55 (1966).
17. Cares, W. R., and Hightower, J. W., *J. Catal.* **23**, 193 (1971); Gibson, M. A., and Hightower, J. W., *J. Catal.* **41**, 420 (1976).
18. Hine, J., "Structural Effects of Equilibria in Organic Chemistry," p. 219. Wiley, New York, 1975.
19. Hanuza, J., and Jeżowska-Trzebiatowksa, B., *J. Mol. Catal.* **4**, 271 (1978).
20. Aso, I., Nakao, M., Egashira, M., Yamazoe, N., and Seiyama, T., *Shokubai* **18**, 106 (1976).
21. Mellor, J. W., "Comprehensive Treatise in Inorganic and Theoretical Chemistry," Vol. VII, p. 482. Longmans, London, 1927.
22. Hattori, T., Ishiguro, A., and Murakami, Y., *J. Inorg. Nucl. Chem.* **40**, 1107 (1978); *Nippon Kagaku Kaishi*, 761 (1977).
23. Clearfield, A., and Stynes, J. A., *J. Inorg. Nucl. Chem.* **26**, 117 (1964).
24. Clearfield, A., and Smith, G. D., *Inorg. Chem.* **8**, 431 (1969).
25. Murakami, Y., and Hayashi, K., *Kogyo Kagaku Zasshi* **72**, 1038 (1969).
26. Dadyburjor, D. B., Jewur, S. S., and Ruckenstein, E., *Catal. Rev.* **19**, 293 (1979).